Synthesis, Luminescence, Electrochemistry, and Ion-Binding Studies of Platinum(II) Terpyridyl Acetylide Complexes

Vivian Wing-Wah Yam,* Rowena Pui-Ling Tang, Keith Man-Chung Wong, and Kung-Kai Cheung

Department of Chemistry, The University of Hong Kong, Pokfulam Road, Hong Kong SAR, People's Republic of China

Received April 24, 2001

A series of platinum(II) terpyridyl acetylide complexes, [Pt(trpy)(C≡CR)]PF_6 (R = C_6H_5, C_6H_4Cl-4, $C_6H_4CH_3$-4, $C_6H_4OCH_3$-4, $C_6H_4NO_2$-4, benzo-15-crown-5, C_6H_3-$(OCH_3)_2$-3,4), have been synthesized and characterized. Their luminescence and electrochemical behaviors have been studied. The ion-binding properties of [Pt(trpy)(C≡C-benzo-15-crown-5)]PF_6 and the X-ray crystal structure of [Pt(trpy)(C≡CC_6H_5)]PF_6 are also reported.

Introduction

The chemistry of square-planar platinum(II) complexes has been extensively studied in the past few decades due to their rich spectroscopic and photophysical behavior,[1−4] as well as their propensity to exhibit weak metal−metal interactions.[2] The platinum(II) terpyridyl complexes have attracted considerable attention in recent years, mainly due to their interesting spectroscopic behavior[3] and useful physical and biological properties.[5] Despite the fact that a number of spectroscopic studies on the platinum(II) terpyridyl systems are known,[3] the utilization of such systems for applications in molecular recognition and chemosensing work is rare,[5a−c,6] in particular, those related to the crown ether-containing platinum(II) systems and their ion-binding properties.[6] The study of crown ethers and other related inclusion compounds in molecular recognition, as well as the design of molecular sensors and probes, has been of growing interest in the field of host−guest chemistry, and important review papers devoted to the chemistry of crown ethers and their analytical, chemical, and biological applications have been published.[7] As a continuation of our studies on the platinum(II) crown ether-containing system,[6] we have synthesized the first platinum(II) alkynyl terpyridyl complex with ethynylbenzo-15-crown-5 as the ligand in this work. Although alkynyl complexes of platinum(II) are known,[4] most of them are confined to platinum(II) phosphines[4a−j] and diimines,[4k−m] with no reports on the platinum(II) terpyridyl system. In addition, a series of noncrown ether-containing analogues have been synthesized to provide insights into the spectroscopic origin of the electronic absorption and emission properties of this class of compounds. Herein are reported the synthesis, electronic absorption, luminescence, electrochemical, and

---

* To whom correspondence should be addressed. Tel: (852)2859-2153. Fax: (852)2857-1586. E-mail: wwyam@hku.hk.

(1) (a) Schindler, J. W.; Fukuda, R. C.; Adamson, A. W. *J. Am. Chem. Soc.* **1982**, *104*, 3596. (b) Biedermann, J.; Gliemann, G.; Klement, U.; Range, K. J.; Zabel, M. *Inorg. Chem.* **1990**, *29*, 1884. (c) Chan, C. W.; Lai, T. F.; Che, C. M.; Peng, S. M. *J. Am. Chem. Soc.* **1993**, *115*, 11245. (d) Miskowski, V. M.; Houlding, V. H.; Che, C. M.; Wang, Y. *Inorg. Chem.* **1993**, *32*, 2518. (e) Yam, V. W. W.; Yeung, P. K. Y.; Cheung, K. K. *J. Chem. Soc., Chem. Commun.* **1995**, 267. (f) Daws, C. A.; Exstrom, C. L.; Sowa, J. R., Jr.; Mann, K. R. *Chem. Mater.* **1997**, *9*, 363. (g) Yersin, H.; Humbs, W.; Strasser, J. *Coord. Chem. Rev.* **1997**, *159*, 325.

(2) (a) Che, C. M.; Butler, L. G.; Gray, H. B. *J. Am. Chem. Soc.* **1981**, *103*, 7796. (b) Rice, S. F.; Gray, H. B. *J. Am. Chem. Soc.* **1983**, *105*, 4571. (c) Miskowski, V. M.; Houlding, V. H. *Inorg. Chem.* **1989**, *28*, 1529. (d) Miskowski, V. M.; Houlding, V. H. *Inorg. Chem.* **1991**, *30*, 4446. (e) Novoa, J. J.; Aullon, G.; Alemany, P.; Alvarez, S. *J. Am. Chem. Soc.* **1995**, *117*, 7169. (f) Tzeng, B. C.; Fu, W. F.; Che, C. M.; Chao, H. Y.; Cheung, K. K.; Peng, S. M. *J. Chem. Soc., Dalton Trans.* **1999**, 1017.

(3) (a) Aldridge, T. K.; Stacy, E. M.; McMillin, D. R. *Inorg. Chem.* **1994**, *33*, 722. (b) Lai, S. W.; Chan, M. C. W.; Cheung, K. K.; Che, C. M. *Inorg. Chem.* **1999**, *38*, 4262. (c) Büchner, R.; Cunningham, C. T.; Field, J. S.; Haines, R.; McMillin, D. R.; Summerton, G. C. *J. Chem. Soc., Dalton Trans.* **1999**, 711. (d) Büchner, R.; Field, J. S.; Haines, R. J.; Cunningham, C. T.; McMillin, D. R. *Inorg. Chem.* **1997**, *36*, 3952. (e) Michalec, J. F.; Bejune, S. A.; McMillin, D. R. *Inorg. Chem.* **2000**, *39*, 2708.

(4) (a) Baralt, E.; Boudreaux, E. A.; Demas, J. N.; Lenhert, P. G.; Lukehart, C. M.; McPhail, D. R.; Myers, J. B., Jr.; Sacksteder, L.; True, W. R. *Organometallics* **1989**, *8*, 2417. (b) Yam, V. W. W.; Chan, L. P.; Lai, T. F. *Organometallics* **1993**, *12*, 2197. (c) Yam, V. W. W.; Yu, K. L.; Cheung, K. K. *J. Chem. Soc., Dalton Trans.* **1999**, 2913. (d) Yam, V. W. W.; Yu, K. L.; Wong, K. M. C.; Cheung, K. K. *Organometallics* **2001**, *20*, 721. (e) Masai, H.; Sonogashira, K.; Hagihara, N. *Bull. Chem. Soc. Jpn.* **1971**, *44*, 2226. (f) Sacksteder, L.; Baralt, E.; DeGraff, B. A.; Lukehart, C. M.; Demas, J. N. *Inorg. Chem.* **1991**, *30*, 3955. (g) Sacksteder, L.; Baralt, E.; DeGraff, B. A.; Lukehart, C. M.; Demas, J. N. *Inorg. Chem.* **1991**, *30*, 2468. (h) Kwok, W. M.; Phillips, D. L.; Yeung, P. K. Y.; Yam, V. W. W. *J. Phys. Chem. A* **1997**, *101*, 9286. (i) Yam, V. W. W.; Yeung, P. K. Y.; Chan, L. P.; Kwok, W. M.; Phillips, D. L.; Yu, K. L.; Wong, R. W. K.; Yan, H.; Meng, Q. J. *Organometallics* **1998**, *17*, 2590. (j) Choi, C. L.; Cheng, Y. F.; Yip, C.; Phillips, D. L.; Yam, V. W. W. *Organometallics* **2000**, *19*, 3192. (k) Chan, C. W.; Cheng, L. K.; Che, C. M. *Coord. Chem. Rev.* **1994**, *132*, 87. (l) Adams, C. J.; James, S. L.; Liu, X.; Raithby, P. R.; Yellowless, L. J. *J. Chem. Soc., Dalton Trans.* **2000**, 63. (m) Hissler, M.; Connick, W. B.; Geiger, D. K.; McGarrah, J. E.; Lipa, D.; Lachicotte, R. J.; Eisenberg, R. *Inorg. Chem.* **2000**, *39*, 447.

(5) (a) Jennette, K. W.; Gill, J. T.; Sadownick, J. A.; Lippard, S. J. *J. Am. Chem. Soc.* **1976**, *98*, 6159. (b) Lippard, S. J. *Acc. Chem. Res.* **1978**, *11*, 211. (c) Peyratout, C. S.; Aldridge, T. K.; Crites, D. K.; McMillin, D. R. *Inorg. Chem.* **1995**, *34*, 4484. (d) Wong, Y. S.; Lippard, S. J. *J. Chem. Soc., Chem. Commun.* **1977**, 824.

(6) Yam, V. W. W.; Tang, R. P. L.; Wong, K. M. C.; Ko, C. C.; Cheung, K. K. *Inorg. Chem.* **2001**, *40*, 571.

(7) (a) Czarnik, A. W. *Fluorescent Chemosensors for Ion and Molecular Recognition*; American Chemical Society: Washington, DC, 1992. (b) Fabbrizzi, L.; Poggi, A. *Chem. Soc. Rev.* **1995**, 197. (c) De Silva, A. P.; Gunaratne, H. Q. N.; Gunnlaugsson, T.; Huxley, A. J. M.; McCoy, C. P.; Rademacher, J. T.; Rice, T. E. *Chem. Rev.* **1997**, *97*, 1515. (d) Yam, V. W. W.; Lo, K. K. W. *Coord. Chem. Rev.* **1999**, *184*, 157.

10.1021/om010336x CCC: $20.00 © 2001 American Chemical Society
Publication on Web 09/22/2001

ion-binding properties of a series of platinum(II) alkynyl terpyridyl complexes. The X-ray crystal structure of [Pt(trpy)(C≡CC$_6$H$_5$)]PF$_6$ has also been determined.

Experimental Section

Materials and Reagents. Dichloro(1,5-cyclooctadiene)platinum(II) and 2,2′:6′,2′′-terpyridine were obtained from Strem Chemicals Inc. Phenylacetylene and (4-chlorophenyl)acetylene were obtained from Aldrich Chemical Co. (4-Methylphenyl)acetylene and (4-methoxyphenyl)acetylene were purchased from Maybridge Chemical Co. Ltd. (4-Nitrophenyl)acetylene,[8] 4-ethynylbenzo-15-crown-5,[9] and (3,4-dimethoxyphenyl)acetylene[9] were synthesized according to literature methods. [Pt(trpy)(MeCN)](OTf)$_2$ was synthesized by modification of the literature method.[3d] All solvents were purified and distilled using standard procedures before use. All other reagents were of analytical grade and were used as received.

[Pt(trpy)(C≡CC$_6$H$_5$)]PF$_6$ (1). To a stirred solution of phenylacetylene (44 mg, 0.43 mmol) in methanol was added sodium hydroxide (23 mg, 0.58 mmol). The resultant solution was stirred at room temperature for 30 min. [Pt(trpy)(MeCN)](OTf)$_2$ (300 mg, 0.39 mmol) was added to the reaction mixture, which turned to a deep red solution immediately and was then stirred for 12 h at room temperature. The mixture was filtered, and a saturated solution of ammonium hexafluorophosphate in methanol was added. The product was isolated, washed with methanol, and dried. Subsequent recrystallization by diffusion of diethyl ether vapor into an acetonitrile solution of the product gave **1** as dark purple crystals. Yield: 60%. ^{1}H NMR (300 MHz, CD$_3$CN, 298 K, relative to Me$_4$Si, δ/ppm): 7.31 (m, 5H, −Ph), 7.55 (t, 2H, J = 6.5 Hz, trpy), 8.13 (m, 7H, trpy), 8.67 (d, 2H, J = 5.1 Hz, trpy). IR (KBr disk, ν/cm^{-1}): 2125 (m), ν(C≡C). Positive ESI-MS: m/z 529 [M − PF$_6$]$^+$, 1203 [2M − PF$_6$]$^+$. Anal. Calcd for C$_{23}$H$_{16}$F$_6$N$_3$PPt: C, 40.90; H, 2.37; N, 6.23. Found: C, 40.87; H, 2.36; N, 6.23.

[Pt(trpy)(C≡CC$_6$H$_4$Cl-4)]PF$_6$ (2). The procedure was similar to that for complex **1**, except (4-chlorophenyl)acetylene (59 mg, 0.43 mmol) was used in place of phenylacetylene. Yield: 59%. ^{1}H NMR (300 MHz, (CD$_3$)$_2$SO, 298 K, relative to Me$_4$Si, δ/ppm): 7.41 (d, 2H, J = 8.3 Hz, −C$_6$H$_4$−), 7.49 (d, 2H, J = 8.3 Hz, −C$_6$H$_4$−), 7.87 (t, 2H, J = 6.5 Hz, trpy), 8.46 (t, 2H, J = 7.6 Hz, trpy), 8.57 (m, 5H, trpy), 9.04 (d, 2H, J = 5.4 Hz, trpy). IR (KBr disk, ν/cm^{-1}): 2120 (m), ν(C≡C). Positive ESI-MS: m/z 564 [M − PF$_6$]$^+$, 1271 [2M − PF$_6$]$^+$. Anal. Calcd for C$_{23}$H$_{15}$ClF$_6$N$_3$PPt: C, 39.98; H, 2.12; N, 5.93. Found: C, 39.95; H, 2.11; N, 5.92.

[Pt(trpy)(C≡CC$_6$H$_4$CH$_3$-4)]PF$_6$ (3). The procedure was similar to that for complex **1**, except (4-methylphenyl)acetylene (51 mg, 0.43 mmol) was used in place of phenylacetylene. Yield: 69%. ^{1}H NMR (300 MHz, CD$_3$CN, 298 K, relative to Me$_4$Si, δ/ppm): 2.41 (s, 3H, −CH$_3$), 7.19 (d, 2H, J = 7.8 Hz, −C$_6$H$_4$−), 7.27 (d, 2H, J = 7.8 Hz, −C$_6$H$_4$−), 7.64 (t, 2H, J = 6.0 Hz, trpy), 8.08 (t, 4H, J = 7.6 Hz, trpy), 8.26 (m, 3H, trpy), 8.90 (d, 2H, J = 5.6 Hz, trpy). IR (KBr disk, ν/cm^{-1}): 2108 (w), ν(C≡C). Positive ESI-MS: m/z 543 [M − PF$_6$]$^+$, 1231 [2M − PF$_6$]$^+$. Anal. Calcd for C$_{24}$H$_{18}$F$_6$N$_3$PPt: C, 41.86; H, 2.62; N, 6.10. Found: C, 41.84; H, 2.65; N, 6.11.

[Pt(trpy)(C≡CC$_6$H$_4$OCH$_3$-4)]PF$_6$ (4). The procedure was similar to that for complex **1**, except (4-methoxyphenyl)acetylene (57 mg, 0.43 mmol) was used in place of phenylacetylene. Yield: 70%. ^{1}H NMR (300 MHz, CD$_3$CN, 298 K, relative to Me$_4$Si, δ/ppm): 3.86 (s, 3H, −OCH$_3$), 6.92 (d, 2H, J = 8.8 Hz, −C$_6$H$_4$−), 7.20 (d, 2H, J = 8.8 Hz, −C$_6$H$_4$−), 7.54 (t, 2H, J = 5.9 Hz, trpy), 7.93 (m, 4H, trpy), 8.15 (m, 3H, trpy), 8.69 (d, 2H, J = 5.0 Hz, trpy). IR (KBr disk, ν/cm^{-1}): 2114 (w), ν(C≡C). Positive ESI-MS: m/z 559 [M − PF$_6$]$^+$, 1263 [2M − PF$_6$]$^+$. Anal. Calcd for C$_{24}$H$_{18}$F$_6$N$_3$OPPt: C, 40.90; H, 2.56; N, 5.96. Found: C, 40.87; H, 2.52; N, 5.94.

[Pt(trpy)(C≡CC$_6$H$_4$NO$_2$-4)]PF$_6$ (5). The procedure was similar to that for complex **1**, except (4-nitrophenyl)acetylene (58 mg, 0.43 mmol) was used in place of phenylacetylene. Yield: 70%. ^{1}H NMR (300 MHz, (CD$_3$)$_2$SO, 298 K, relative to Me$_4$Si, δ/ppm): 7.68 (d, 2H, J = 8.9 Hz, −C$_6$H$_4$−), 8.23 (d, 2H, J = 8.9 Hz, −C$_6$H$_4$−), 7.85 (t, 2H, J = 6.6 Hz, trpy), 8.46 (t, 2H, J = 7.9 Hz, trpy), 8.55 (m, 5H, trpy), 8.98 (d, 2H, J = 5.6 Hz, trpy). IR (KBr disk, ν/cm^{-1}): 2117 (s), ν(C≡C). Positive ESI-MS: m/z 573 [M − PF$_6$]$^+$, 1291 [2M − PF$_6$]$^+$. Anal. Calcd for C$_{23}$H$_{14}$F$_6$N$_4$O$_2$PPt: C, 38.44; H, 1.95; N, 7.80. Found: C, 38.46; H, 1.92; N, 7.65.

[Pt(trpy)(C≡C-benzo-15-crown-5)]PF$_6$ (6). The procedure was similar to that for complex **1**, except 4-ethynylbenzo-15-crown-5 (130 mg, 0.45 mmol) and triethylamine (60 mg, 0.59 mmol) was used in place of phenylacetylene and sodium hydroxide. Yield: 73%. ^{1}H NMR (300 MHz, CD$_3$CN, 298 K, relative to Me$_4$Si, δ/ppm): 3.65 (m, 8H, −OCH$_2$−), 3.85 (m, 4H, −OCH$_2$−), 4.10 (m, 4H, C$_6$H$_3$OCH_2−), 6.78 (s, 1H, −C$_6$H$_3$−), 6.87 (d, 2H, J = 4.0 Hz, −C$_6$H$_3$−), 7.59 (t, 2H, J = 6.6 Hz, trpy), 7.97 (m, 4H, trpy), 8.21 (m, 3H, trpy), 8.75 (d, 2H, J = 4.9 Hz, trpy). IR (KBr disk, ν/cm^{-1}): 2116 (w), ν(C≡C). Positive ESI-MS: m/z 719 [M − PF$_6$]$^+$, 1583 [2M − PF$_6$]$^+$. Anal. Calcd for C$_{31}$H$_{30}$N$_3$O$_5$PtPF$_6$: C, 43.06; H, 3.47; N, 4.86. Found: C, 43.11; H, 3.46; N, 4.91.

[Pt(trpy)(C≡CC$_6$H$_3$-(OCH$_3$)$_2$-3,4)]PF$_6$ (7). The procedure was similar to that for complex **1**, except (3,4-dimethoxyphenyl)acetylene (70 mg, 0.43 mmol) was used in place of phenylacetylene. ^{1}H NMR (300 MHz, CD$_3$CN, 298 K, relative to Me$_4$Si, δ/ppm): 3.87 (s, 3H, −OCH$_3$), 3.89 (s, 3H, −OCH$_3$), 6.95 (m, 3H, −C$_6$H$_3$−), 7.69 (t, 2H, J = 6.7 Hz, trpy), 8.12 (t, 4H, J = 8.5 Hz, trpy), 8.30 (m, 3H, trpy), 8.99 (d, 2H, J = 5.1 Hz, trpy). IR (KBr disk, ν/cm^{-1}): 2109 (w), ν(C≡C). Positive ESI-MS: m/z 589 [M − PF$_6$]$^+$, 1323 [2M − PF$_6$]$^+$. Anal. Calcd for C$_{25}$H$_{20}$F$_6$N$_3$O$_2$PPt: C, 40.87; H, 2.72; N, 5.72. Found: C, 40.81; H, 2.76; N, 5.91.

Physical Measurements and Instrumentation. UV/vis spectra were obtained on a Hewlett-Packard 8452A diode array spectrophotometer, IR spectra as KBr disks on a Bio-Rad FTS-7 Fourier transform infrared spectrophotometer (4000−400 cm^{-1}), and steady-state excitation and emission spectra on a Spex Fluorolog 111 spectrofluorometer. Solid-state photophysical studies were carried out with solid samples contained in a quartz tube inside a quartz-walled Dewar flask. Measurements of the butyronitrile glass or solid-state samples at 77 K were similarly conducted with liquid nitrogen filled in the optical Dewar flask. Excited-state lifetimes of solution samples were measured using a conventional laser system. The excitation source was the 355 nm output (third harmonic, 8 ns) of a Spectra-Physics Quanta-Ray Q-switched GCR-150 pulsed Nd:YAG laser (10 Hz). For self-quenching studies, the rate constants of emission decay ($k_{\text{obsd}} = 1/\tau$) are well modeled by the Stern−Volmer expression (eq 1):

$$k_{\text{obsd}} = k_{\text{q}}[\text{Pt}] + k_0 \qquad (1)$$

where k_{q} is the self-quenching rate constant, [Pt] is the concentration of the platinum complex, and $k_0 = 1/\tau_0$ is the rate constant of excited-state decay at infinite dilution. Luminescence quantum yields were measured by the optical dilute method reported by Demas and Crosby.[10a] The luminescence quantum yield of the sample was determined according to eq 2

---

(8) Takahashi, S.; Kuroyama, Y.; Sonogashira, K.; Hagihara, N. *Synthesis* **1980**, 627.

(9) Kikukawa, K.; He, G. X.; Abe, A.; Goto, T.; Arata, R.; Ikeda, T.; Wada, F.; Matsuda, T. *J. Chem. Soc., Perkin Trans. 2* **1987**, 135.

(10) (a) Demas, J. N.; Crosby. G. A. *J. Phys. Chem.* **1971**, *75*, 991. (b) van Houten, J.; Watts, R. *J. Am. Chem. Soc.* **1976**, *98*, 4853.

$$\phi_s = \phi_r(B_r/B_s)(n_s/n_r)^2(D_s/D_r) \quad (2)$$

where the subscripts s and r refer to the sample and reference solutions, respectively, $B = 1 - 10^{-AL}$, A is the absorbance at the excitation wavelength, L is the path length, n is the refractive index of the solvent, and D is the integrated emission intensity. A degassed aqueous solution of $[Ru(bpy)_3]Cl_2$ ($\phi_{em} = 0.042$, excitation wavelength at 436 nm) was used as the reference.[10b]

All solutions for photophysical studies were degassed on a high-vacuum line in a two-compartment cell consisting of a 10 mL Pyrex bulb and a 1 cm path length quartz cuvette sealed from the atmosphere by a Bibby Rotaflo HP6 Teflon stopper. The solutions were subject to no less than four freeze−pump−thaw cycles.

^1H NMR spectra were recorded on a Bruker DPX-300 FT-NMR spectrometer (300 MHz) in CD_3CN or $(CD_3)_2SO$ at 298 K, and chemical shifts are reported relative to Me_4Si. Positive ESI mass spectra were recorded on a Finnigan LCQ mass spectrometer. Elemental analyses of the new complexes were performed on a Carlo Erba 1106 elemental analyzer at the Institute of Chemistry, Chinese Academy of Sciences. Cyclic voltammetric measurements were performed by using a CH Instruments, Inc. Model CHI 620 electrochemical analyzer, which was interfaced to an IBM-compatible 486 personal computer. The electrolytic cell used was a conventional two-compartment cell. Electrochemical measurements were performed in acetonitrile solutions with 0.1 M $^nBu_4NPF_6$ (TBAH) as supporting electrolyte at room temperature. The reference electrode was a $Ag/AgNO_3$ (0.1 M in acetonitrile) electrode, and the working electrode was a glassy-carbon (Atomergic Chemetal V25) electrode with a piece of platinum wire as counter electrode in a compartment which is separated from the working electrode by a sintered-glass frit. The ferrocenium/ferrocene couple ($FeCp_2{}^{+/0}$) was used as the internal reference. All solutions for electrochemical studies were deaerated with prepurified argon gas just before measurements. Treatment of the electrode surfaces was as reported elsewhere.[11]

The electronic absorption spectral titration for binding constant determination was performed with a Hewlett-Packard 8452A diode array spectrophotometer at 25 °C which was controlled by a Lauda RM6 compact low-temperature thermostat. Supporting electrolyte (0.1 mol dm^{-3} $^nBu_4NPF_6$) was added to maintain a constant ionic strength of the sample solution, in order to avoid any changes arising from a change in the ionic strength of the medium. Binding constants for 1:1 complexation were obtained by a nonlinear least-squares fit[12] of the absorbance (X) vs the concentration of the metal ion added ($[M^{n+}]$) according to eq 3

$$X = X_0 + \frac{X_{lim} - X_0}{2[Pt]_T}\{[Pt]_T + [M^{n+}] + 1/K_S - [([Pt]_T + [M^{n+}] + 1/K_S)^2 - 4[Pt]_T\,[M^{n+}]]^{1/2}\} \quad (3)$$

where X_0 and X are the absorbances of complex **6** at a selected wavelength in the absence and presence of the metal cation, respectively, $[Pt]_T$ is the total concentration of complex **6**, $[M^{n+}]$ is the concentration of the metal cation M^{n+}, X_{lim} is the limiting value of the absorbance in the presence of excess metal ion, and K_S is the stability constant.

For systems involving Pt:M^{n+} complexation in both 1:1 and 2:1 complexation stoichiometries, the binding constants were determined by using eq 4[6]

$$K_{11} = \frac{[Pt{\cdot}M^{n+}]}{[Pt]_1[M^{n+}]}$$

$$K_{21} = \frac{[Pt_2{\cdot}M^{n+}]}{[Pt{\cdot}M^{n+}]\,[Pt]_1}$$

$$[Pt]_T = [Pt]_1 + [Pt{\cdot}M^{n+}] + [Pt_2{\cdot}M^{n+}]$$

$$[Pt]_T = \frac{[Pt{\cdot}M^{n+}]}{K_{11}[M^{n+}]} + [Pt{\cdot}M^{n+}] + \frac{K_{21}[Pt{\cdot}M^{n+}]^2}{K_{11}[M^{n+}]}$$

$$[Pt{\cdot}M^{n+}] = \frac{a}{2K_{21}}$$

where

$$a = -1 - K_{11}[M^{n+}] + [(1 + K_{11}[M^{n+}])^2 + 4K_{21}K_{11}[M^{n+}][Pt]_T]^{1/2}$$

$$[Pt]_1 = \frac{a}{2K_{21}K_{11}[M^{n+}]}$$

$$[Pt_2{\cdot}M^{n+}] = \frac{a^2}{4K_{21}K_{11}[M^{n+}]}$$

$$X = \frac{X_0}{[Pt]_T}[Pt]_1 + \frac{X_{lim}}{[Pt]_T}[Pt{\cdot}M^{n+}] + \frac{2X_{lim}}{[Pt]_T}[Pt_2{\cdot}M^{n+}] \quad (4)$$

where $[Pt]_1$ is the concentration of complex **6** in the unbound state, $[Pt{\cdot}M^{n+}]$ and $[Pt_2{\cdot}M^{n+}]$ are the concentrations of the 1:1 and 2:1 ion-bound adducts, respectively, and K_{11} and K_{21} are the respective stability constants for 1:1 and 2:1 complexation. It is assumed that the molar extinction coefficient of the 2:1 ion-bound adduct, ($Pt_2{\cdot}M^{n+}$), is twice that of the 1:1 adduct form, ($Pt{\cdot}M^{n+}$).

Crystal Structure Determination. Single crystals of **1** were obtained by vapor diffusion of diethyl ether into an acetonitrile solution of the complex. All the experimental details are given in Table 1. A purple crystal of dimensions 0.35 × 0.07 × 0.07 mm in a glass capillary was used for data collection at 28 °C on a Rigaku AFC7R diffractometer. The space group was determined on the basis of systematic absences and on a statistical analysis of intensity distribution, and the successful refinement of the structure was solved by Patterson methods and expanded by Fourier methods (PATTY[13]) and refinement by full-matrix least squares using the software package TeXsan[14] on a Silicon Graphics Indy computer. One crystallographic asymmetric unit consists of one formula unit with the non-H atoms of CH_3CN at special positions. The F atoms of $PF_6{}^-$ were disordered and were placed at 10 positions, with F(1)−F(10) having occupation numbers of 0.8, 1.0, 0.45, 0.8, 0.8, 0.45, 0.5, 0.5, 0.3, and 0.4, respectively. In the least-squares refinement, all 27 non-H atoms of the cation and P(1) were refined anisotropically, the disordered F atoms and the non-H atoms of CH_3CN were refined isotropically, and 16 H atoms at calculated positions with thermal parameters equal to 1.3 times that of the attached C atoms were not refined. H atoms bonded to the disordered methyl C atom in CH_3CN were not included in the calculation. The final difference Fourier map was featureless, with maximum positive and negative peaks of 0.90 and 0.53 e Å^{-3}, respectively.

---

(11) Che, C. M.; Wong, K. Y.; Anson, F. C. *J. Electroanal. Chem. Interfacial Electrochem.* **1987**, *226*, 221.

(12) Bourson, J.; Pouget, J.; Valeur, B. *J. Phys. Chem.* **1993**, *97*, 4552.

(13) PATTY: Beurskens, P. T.; Admiraal, G.; Beurskens, G.; Bosman, W. P.; Garcia-Granda, S.; Gould, R. O.; Smits, J. M. M.; Smykalla, C. The DIRDIF Program System; Technical Report of the Crystallography Laboratory; University of Nijmegen, Nijmegen, The Netherlands, 1992.

(14) TeXsan: Crystal Structure Analysis Package; Molecular Structure Corp., The Woodlands, TX, 1985 and 1992.

Table 1. Crystal and Structure Determination Data for 1

mol formula	$(C_{23}H_{16}N_3Pt)^+PF_6^-\cdot 0.5CH_3CN$
fw	694.98
cryst color	purple
cryst size (mm)	0.35 × 0.07 × 0.07
cryst syst	monoclinic
space group	*C*2/*c* (No. 15)
a (Å)	19.614(3)
b (Å)	20.62(2)
c (Å)	13.405(2)
β (deg)	117.60(1)
V (Å^3)	4805(2)
Z	8
F(000)	2604
μ (cm^{-1})	59.49
calcd density (g cm^{-3})	1.921
T (K)	301
diffractometer	AFC7R
λ, (Å, graphite monochromated, Mo Kα)	0.710 73
collecn range (deg)	$2\theta_{max} = 50$ (*h*, 0−23; *k*, 0−24; *l*, −15 to +14)
scan mode; scan speed (deg min^{-1})	$\omega-2\theta$; 8
scan width (deg)	$0.63 + 0.35 \tan\theta$
R^a	0.038
$R_w{}^a$	0.047
max shift $(\Delta/\sigma)_{max}$	0.05
goodness of fit	1.74
no. of data collected	4496
no. of unique data	4360
no. of data used in refinement	2242
no. of params refined	146
residual extrema in final diff map (e Å^{-3})	0.09, 0.53

[a] $w = 4F_o{}^2/\sigma^2(F_o{}^2)$, where $\sigma^2(F_o{}^2) = \sigma^2(I) + (0.02F_o{}^2)^2$ with $I > 3\sigma(I)$.

Scheme 1. Synthetic Route of Complexes 1−7

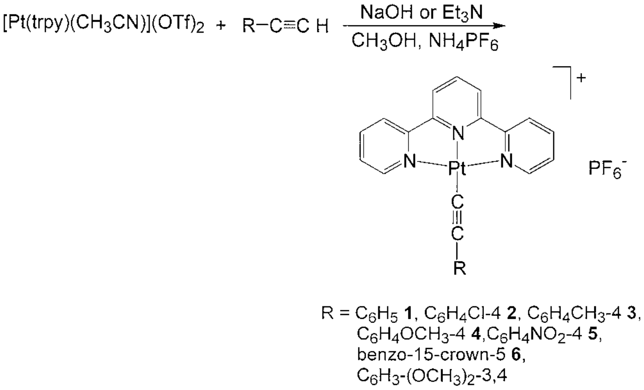

Results and Discussion

Synthesis. The synthetic route for the formation of platinum(II) terpyridyl acetylide complexes is summarized in Scheme 1. The starting material [Pt(trpy)(MeCN)](OTf)$_2$ was synthesized by modification of literature procedures[3d] using a large excess of AgOTf and a much higher reaction temperature. Reaction of [Pt(trpy)(MeCN)](OTf)$_2$ with HC≡CR in methanol in the presence of sodium hydroxide at room temperature, followed by metathesis reaction using NH_4PF_6 and subsequent recrystallization from MeCN−Et_2O, afforded **1**−**5** and **7** as dark red to dark purple crystals. For complex **6**, the synthetic method is similar, except that triethylamine was used as the deprotonating agent instead of sodium hydroxide in order to prevent the binding of sodium ion into the crown cavity. The identities of all the complexes have been confirmed by IR spectroscopy, satisfactory elemental analyses, ^{1}H NMR spectroscopy, and ESI-mass spectrometry. The crystal structure of [Pt(trpy)(C≡CC$_6$H$_5$)]PF$_6$ **1** has also been determined.

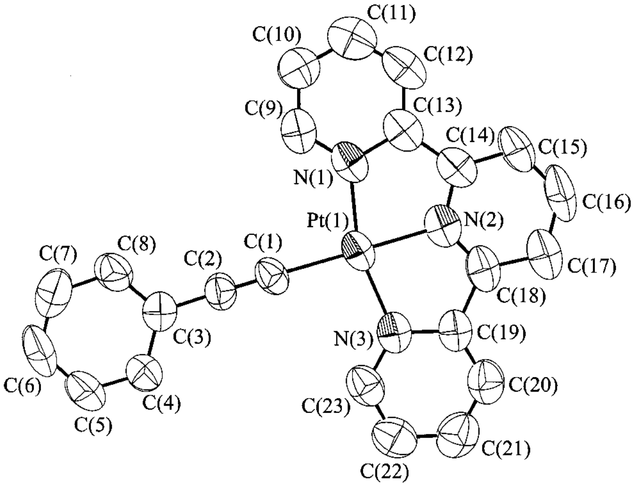

Figure 1. Perspective drawing of the complex cation of **1** with atomic numbering. Thermal ellipsoids were shown at the 40% probability level.

Table 2. Selected Bond Distances (Å) and Bond Angles (deg) for 1

Pt(1)−N(1)	2.01(1)	Pt(1)−C(1)	1.98(1)
Pt(1)−N(2)	1.97(10)	C(1)−C(2)	1.19(1)
Pt(1)−N(3)	2.03(1)		
N(1)−Pt(1)−N(2)	80.6(5)	N(1)−Pt(1)−C(1)	99.5(5)
N(2)−Pt(1)−N(3)	81.0(4)	N(3)−Pt(1)−C(1)	98.9(5)
N(1)−Pt(1)−N(3)	161.6(4)	Pt(1)−C(1)−C(2)	179.0(1)
N(2)−Pt(1)−C(1)	178.8(4)		

Crystal Structure Determination. The perspective drawing of the complex cation of **1** is shown in Figure 1. Selected bond distances and angles are tabulated in Table 2. The coordination geometry about platinum is essentially square planar with the bond distance of the platinum to central nitrogen atom of the terpyridine ligand slightly shorter than that to the other two outer nitrogen atoms, as is required by the steric demand of the terpyridine ligand. All the Pt−N distances are in the range found for typical platinum terpyridine complexes.[2f,3a−d] Not surprisingly, the N−Pt−N angles (N(1)−Pt(1)−N(2), 80.6°; N(2)−Pt(1)−N(3), 81.0°; N(1)−Pt(1)−N(3), 161.6°) deviate from the idealized values of 90 and 180° as a consequence of the geometric constraints imposed by terpyridine ligands. The Pt−C bond distance is 1.98 Å, which compares well with a value of 1.95 Å for the platinum bis(acetylide) diimine complexes.[4l,m] The C≡C bond length of 1.19 Å is comparable to those of other related platinum(II) acetylide complexes.[4a−d,l,m] The phenyl ring of the acetylide ligand is almost parallel to the plane of platinum−terpyridine with a dihedral angle of 5.6°. The crystal packing of **1** revealed a head-to-tail stacking between pairs of complex cations (Figure 2). The intermolecular Pt···Pt distance of 3.36−3.38 Å is suggestive of intermolecular interaction between the two metal centers.

Electronic Absorption Spectroscopy. The electronic absorption spectra of complexes **1**−**7** in acetoni-

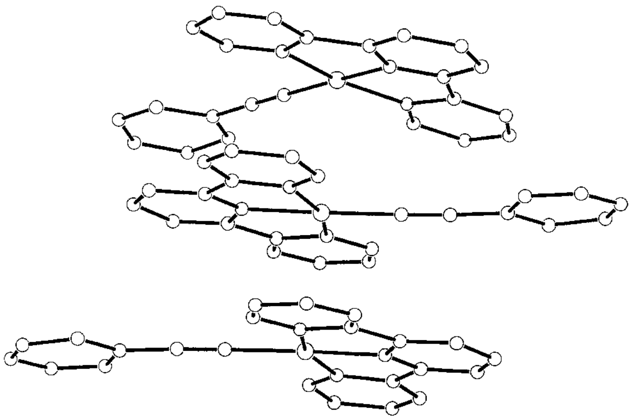

Figure 2. Crystal packing diagram of **1**.

Table 3. Photophysical Spectral Data for 1−7

	absorption[a] λ_{abs}/nm (ϵ/dm^3 mol^{-1} cm^{-1})	emission medium (T/K)	emission λ_{em}/nm[b] (τ_0/μs[c])	ϕ_{em}[d]
1	272 (33 410), 286 (23 860), 312 (12 450), 28 (12 280), 342 (14 440), 432 (4430)	CH_3CN (298)	630 (0.5)	0.0124
		solid (298)	800 (<0.1)	
		solid (77)	830 (0.7)	
		glass[e] (77)	530 (13.3)	
2	272 (36 550), 286 (27 830), 312 (12 530), 328 (12 490), 342 (14 500), 432 (4790)	CH_3CN (298)	620 (0.5)	0.0073
		solid (298)	710 (<0.1)	
		solid (77)	790 (0.8)	
		glass[e] (77)	530 (15.0)	
3	272 (36 150), 312 (12 380), 330 (12 390), 344 (13 870), 412 sh (3580), 456 (4380)	CH_3CN (298)	665 (0.1)	0.0015
		solid (298)	720 (<0.1)	
		solid (77)	740 (1.0)	
		glass[e] (77)	545 (13.8)	
4	272 (39 310), 308 (13 920), 330 (13 500),344 (13 140), 416 sh (3500), 474 (4700)	CH_3CN (298)	–[f]	
		solid (298)	–[f]	
		solid (77)	–[f]	
		glass[e] (77)	580 (11.8)	
5	272 (33 500), 286 (23 780), 310 (24 500), 326 (12 360), 340 (14 640), 417 (9740)	CH_3CN (298)	560 (<0.1)	0.0011
		solid (298)	720 (<0.1)	
		solid (77)	790 (0.7)	
		glass[e] (77)	510 (240)	
6	288 (31 440), 308 (14 910), 330 (14 710), 344 (13 940), 412 sh (2910), 476 (4180)	CH_3CN (298)	–[f]	
		solid (298)	–[f]	
		solid (77)	–[f]	
		glass[e] (77)	585 (9.9)	
7	286 (40 690), 308 (19 000), 330 (15 780), 344 (15 760), 412 sh (3890), 480 (5690)	CH_3CN (298)	–[f]	
		solid (298)	–[f]	
		solid (77)	–[f]	
		glass[e] (77)	590 (9.3)	

[a] In acetonitrile at 298 K. [b] Emission maxima are corrected values. [c] τ_0 is the lifetime at infinite dilution. [d] The luminescence quantum yield, measured at room temperature using $[Ru(bpy)_3]^{2+}$ as a standard. [e] In butyronitrile glass (concentration 5×10^{-6} mol dm^{-3}). [f] Nonemissive.

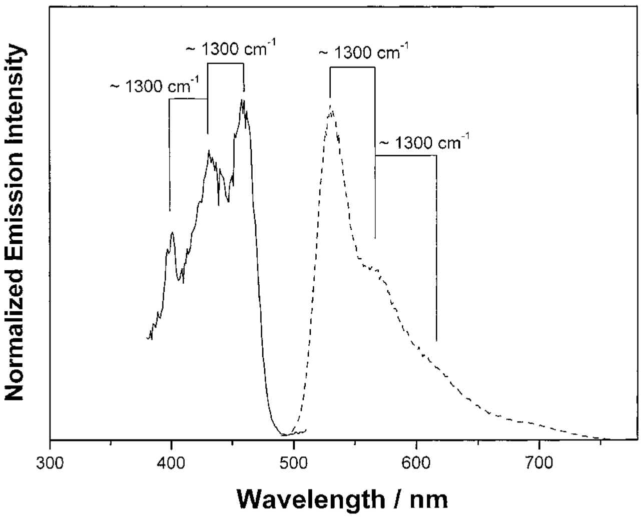

Figure 3. Emission (---) and excitation (—) spectra of **1** in butyronitrile glass at 77 K.

trile solution exhibited intense vibronic-structured absorption bands at 300−350 nm with extinction coefficients (ϵ) on the order of 10^4 dm^3 mol^{-1} cm^{-1} and a less intense band at ca. 456−480 nm with ϵ on the order of 10^3 dm^3 mol^{-1} cm^{-1} (Table 3). With reference to previous spectroscopic work on platinum(II) terpyridine complexes,[3a−c] the absorption bands at 300−350 nm are most probably derived from the intraligand (IL) transition of the terpyridine ligands, while the low-energy absorption band at 456−480 nm is tentatively assigned to the dπ(Pt) → π*(trpy) metal-to-ligand charge transfer (MLCT) transition. Complex **5**, with the most electron-withdrawing nitro group on the acetylide, shows an absorption band at 456 nm, which is at the highest energy among the complexes. In general, the stronger the electron-donating ability of the acetylide ligand is, the lower will be the energy of the low-energy absorption. This observation is in line with an MLCT assignment of the low-energy absorption band, since electron-rich substituents on the phenyl ring of the acetylide ligand would render the platinum metal center more electron-rich and hence raise the dπ(Pt) orbital energy, leading to a lower energy MLCT absorption. Although an assignment of an acetylide-to-terpyridine ligand-to-ligand charge transfer (LLCT) transition would also give rise to such an energy trend, an assignment of MLCT transition is favored, probably with some mixing of LLCT character. The absorption spectral properties of the complexes were found to obey Beer's law in the concentration range 10^{-5}−10^{-2} mol dm^{-3} in dimethylformamide solution, suggesting the lack of any significant occurrence of complex aggregation.

Emission Properties. All the complexes show emission properties in 77 K butyronitrile glass, while at room temperature in acetonitrile solutions, all complexes except **4**, **6**, and **7** were found to exhibit luminescence (Table 3). The large Stokes shifts and observed lifetimes in the microsecond range for their emissions are suggestive of a triplet parentage. The butyronitrile glass of complexes **1**−**5** upon excitation at $\lambda > 350$ nm show well-resolved vibronic structured emissions at 510−580 nm with progressional spacings of ca. 1300 cm^{-1}, which correspond to the aromatic vibrational mode of the terpyridine ligands. Figure 3 shows the excitation and emission spectra for **1** in 77 K butyronitrile glass. The emission energies of the complexes in solution were found to depend on the nature of the substituents on the phenyl ring of the acetylide ligands. Complex **3**, which bears the electron-rich methyl substituent, shows the lowest emission energy, while complex **5**, with the most electron-poor nitro group, shows the highest emission energy (Figure 4). This trend is consistent with a ^{3}MLCT assignment. A shift in the emission energies to the red was observed upon going from acetonitrile solutions to the solid state at room temperature with the exception of **4**, **6**, and **7** which were nonemissive in solutions at 298 K. Such low-energy emissions at ca. 690−800 nm in the solid state are assigned as derived

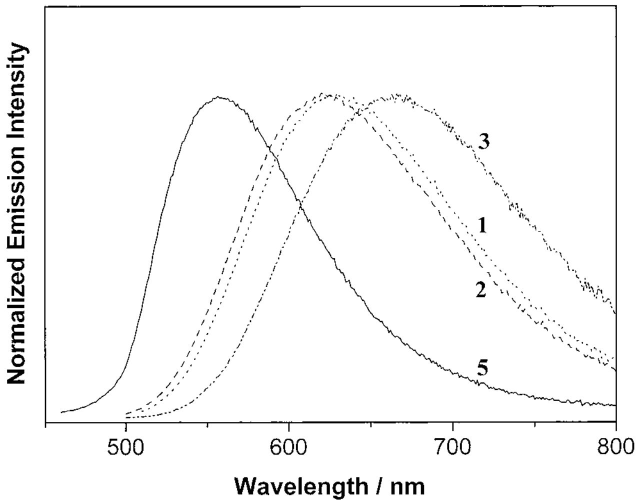

Figure 4. Normalized solution emission spectra of **1** (··· ···), **2** (---), **3** (·· — ··), and **5** (—), in acetonitrile at 298 K.

Table 4. Electrochemical Data for 1−7[a]

Complex	oxidation E_{pa}/V vs SCE[b]	reduction $E_{1/2}$/V vs SCE[c]
1	+1.22	−0.97 −1.46
2	+1.28	−1.00 −1.46
3	+1.25	−1.03 −1.45
4	+1.02	−1.05 −1.46
5	+1.46	−1.18 −1.45
6	+0.96	−1.06 −1.45
7	+1.02	−1.08 −1.45

[a] In acetonitrile solution with 0.1 M $^{n}Bu_4NPF_6$ (TBAH) as supporting electrolyte at room temperature; scan rate 100 mV s^{-1}. [b] E_{pa} refers to the anodic peak potential for the irreversible oxidation waves. [c] $E_{1/2} = (E_{pa} + E_{pc})/2$; E_{pa} and E_{pc} are peak anodic and peak cathodic potentials, respectively.

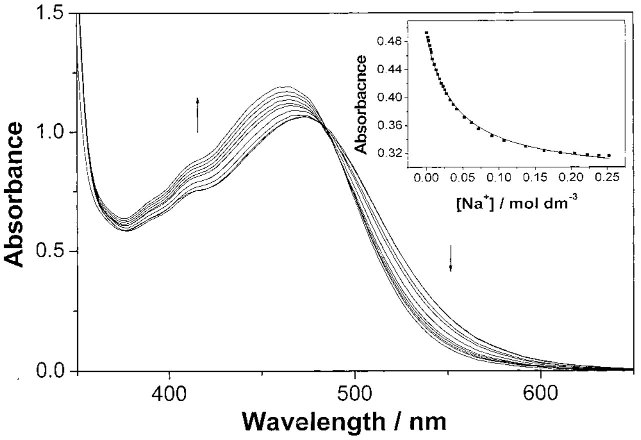

Figure 5. Electronic absorption spectral traces of **6** (2.6×10^{-4} mol dm^{-3}) in dimethylformamide (0.1 mol dm^{-3} $^{n}Bu_4NPF_6$) upon addition of $NaClO_4$ (path length = 1 cm). The insert shows a plot of absorbance vs [Na^+] monitored at $\lambda = 530$ nm (■) and its theoretical fit (—).

from triplet states of metal−metal bond-to-ligand charge transfer (MMLCT) character, resulting from the significant Pt···Pt interaction in the solid state. When the temperature is lowered to 77 K, the emission band in the solid state shows a further red shift in emission energies, which may be rationalized by the lattice contraction at low temperatures, leading to a shortening of the Pt···Pt intermolecular separation and, hence, an increased Pt···Pt interaction. The self-quenching rate constants for complexes **1**−**3** at room temperature are 1.73, 1.74, and 1.45×10^9 dm^3 mol^{-1} s^{-1}, respectively.

Electrochemical Properties. The electrochemical data for complexes **1**−**7** are summarized in Table 4. All the complexes show two quasi-reversible couples at ca. −1.05 and −1.45 V vs SCE. The relative insensitivity of the potentials toward the nature of the acetylide ligands with different substituents on the phenyl ring suggests that these couples probably arise mainly from the terpyridine-based reductions with some mixing of the Pt(II) metal character. Similar assignment has also been suggested in other platinum terpyridyl systems.[15] Irreversible anodic waves are noted at ca. +1.02 to +1.46 V vs. SCE. With reference to the previous studies on other platinum complexes,[16] metal-centered oxidation from Pt(II) to Pt(III) is tentatively assigned. The oxidation of complex **5** occurs at a more positive potential than the others, which may be ascribed to the presence of the most electron-withdrawing nitro group on the phenylacetylide ligand, which lowers the energy of the dπ(Pt) orbital. Thus, complex **5** is most difficult to be oxidized among all the complexes studied.

Cation-Binding Properties. Upon addition of alkali-metal cations to a dimethylformamide solution of **6**, the MLCT absorption band exhibits a blue shift in absorption energy. Figure 5 shows the UV−visible absorption spectral traces upon addition of sodium cations to a solution of **6**, in which a well-defined isosbestic point was observed. Spectrochemical recognition of guest metal ions is confirmed by the absence of changes in the absorption bands of the control complex **7**. For binding of Na^+, a log K_S value of 1.40(±0.01) was obtained according to eq 3. The 1:1 stoichiometry for Na^+ ion binding is evidenced by the close agreement of the experimental data with the theoretical fit (Figure 5, insert) and has further been confirmed by the method of continuous variation,[17] where a break point at a mole fraction **6**/(**6** + Na^+) of 0.5 is observed. The much smaller binding constant of **6** compared to that of a related [Pt(trpy)(S-benzo-15-crown-5)]PF_6 complex in acetonitrile[6] may be attributed to the difference in polarity of the solvent. Since dimethylformamide is much more polar than acetonitrile, the metal cations are already well solvated or stabilized by the solvent molecules. The binding of the cations in the crown cavity is therefore less favored, leading to smaller binding constants. This solvent effect on cation binding has also been reported for other crown ether-containing compounds.[18] In the case of K^+, complexes with stoichiometries of both 2:1 and 1:1 were formed. This binding mode is supported

---

(15) (a) Hill, M. G.; Bailey, J. A.; Miskowski, V. M.; Gray, H. B. *Inorg. Chem.* **1996**, *35*, 4585. (b) Crites, D. K.; Cunningham, C. T.; McMillin, D. R. *Inorg. Chim. Acta* **1998**, *273*, 346.

(16) (a) Blanton, C. B.; Murtaza, Z.; Shaver, R. J.; Rillema, D. P. *Inorg. Chem.* **1992**, *31*, 3230. (b) von Zelewsky, A.; Gremaud, G. *Helv. Chim. Acta* **1988**, *84*, 85.

(17) (a) Jaffe, H. H.; Orchin, M. *Theory and Applications of Ultraviolet Spectroscopy*; Wiley: New York, 1962. (b) Peyman, A.; Uhlmann, E.; Wagner, K.; Augustin, S.; Weiser, C.; Will, D. W.; Breipohl, G. *Angew. Chem., Int. Ed. Engl.* **1997**, *36*, 2809.

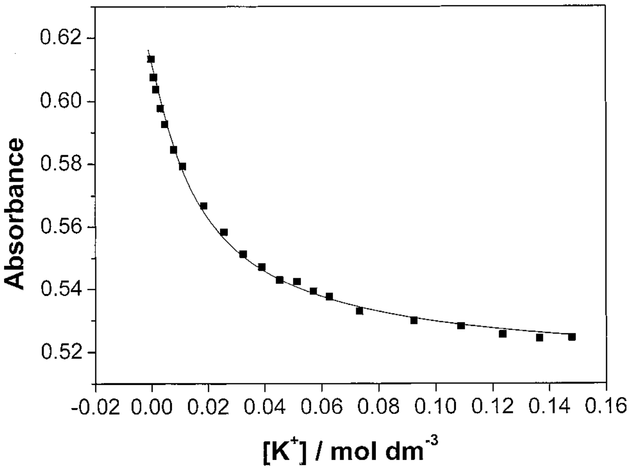

Figure 6. Plot of absorbance of **6** (2.5×10^{-4} mol dm^{-3}) in dimethylformamide (0.1 mol dm^{-3} $^{n}Bu_4NPF_6$) vs [K$^+$] monitored at $\lambda = 520$ nm (■) and its theoretical fit (—).

by the close resemblance of the experimental data with the theoretical fit (Figure 6) and also the lack of well-defined isosbestic points on the UV−visible spectral traces. Log K_{11} and log K_{21} values of 1.99(±0.05) and 2.79(±0.05) were obtained, respectively, according to eq 4. However, no satisfactory fit for eqs 3 and 4 can be obtained for the binding studies of Ba^{2+}. The blue shift in absorption energies observed upon ion binding is consistent with the MLCT assignment of the low-energy absorption, since a reduced electron-donation ability of the acetylide would occur upon ion binding, causing the MLCT to occur at higher energies.

The ion-binding studies have further been confirmed by positive ESI mass spectrometry. A 1:1 adduct was observed for the binding of **6** with Na$^+$ and Ba^{2+}, while for K$^+$, both 1:1 and 2:1 adducts were observed (Table 5). This is fully consistent with the binding properties studied by UV−visible spectroscopy. Similar to the absorption studies, control experiments with the crown-free analogue **7** did not show the presence of such ion-bound species upon the addition of metal ions, providing further supporting evidence for the binding of cations to the crown moieties.

Conclusion

A series of platinum(II) terpyridyl acetylide complexes were successfully synthesized and shown to exhibit long-lived emissive states. The emission energies in acetonitrile at room temperature were found to depend on the nature of the acetylide ligands with different substituents on the phenyl ring, i.e., the more electron-withdrawing the group on the phenylacetylide ligand is, the higher is the emission energy. This trend is consistent with an assignment of a triplet metal-to-terpyridine metal-to-ligand charge transfer (^{3}MLCT) state, probably mixed with some acetylide-to-terpyridine ligand-to-ligand charge transfer (^{3}LLCT) character. From the electrochemical studies, all the complexes showed two quasi-reversible terpyridine-based reduction couples with some mixing of the Pt(II) metal character and one irreversible metal-based oxidation wave. The cation-binding properties for a crown ether-containing complex have also been studied. The spectral change upon addition of guest metal ions was monitored by electronic absorption studies. For Na$^+$, a 1:1 binding mode with log K_S of 1.40(±0.01) was observed, while for K$^+$, both complexes with stoichiometries of 2:1 and 1:1 were formed with log K_{11} and log K_{21} of 1.99(±0.05) and 2.79(±0.05), respectively. The ion-binding properties have further been confirmed by positive ESI mass spectrometry.

Table 5. Ion Clusters Observed in the Positive ESI Mass Spectra of 6 with $NaClO_4$, KPF_6, and $BaClO_4$ in Acetonitrile Solution

m/*z*	ion cluster
842	$\{[Pt(trpy)(C{\equiv}C\text{-benzo-15-crown-5})\cdot Na]ClO_4\}^+$
903	$\{[Pt(trpy)(C{\equiv}C\text{-benzo-15-crown-5})\cdot K]PF_6\}^+$
1767	$\{\{[Pt(trpy)(C{\equiv}C\text{-benzo-15-crown-5})]_2\cdot K\}(PF_6)_2\}^+$
1055	$\{[Pt(trpy)(C{\equiv}C\text{-benzo-15-crown-5})\cdot Ba](ClO_4)_2\}^+$

Acknowledgment. V.W.-W.Y. acknowledges support from The University of Hong Kong and the receipt of a Croucher Senior Research Fellowship (2000−2001) from the Croucher Foundation. The work described in this paper has fully been supported by a grant from the Research Grants Council of the Hong Kong Special Administrative Region, People's Republic of China (Project No. HKU 7123/00P). R.P.-L.T. acknowledges the receipt of a postgraduate studentship, administered by The University of Hong Kong, and K.M.-C.W. the receipt of a University Postdoctoral Fellowship from The University of Hong Kong.

Supporting Information Available: Tables giving atomic coordinates, anisotropic thermal parameters, bond lengths, and bond angles for complex **1**. This material is available free of charge via the Internet at http://pubs.acs.org.

OM010336X

---

(18) (a) Frensdorf, H. K. *J. Am. Chem. Soc.* **1971**, *93*, 600. (b) Kauffmann, E.; Lehn, J. M.; Sauvage, J. P.; *Helv. Chim. Acta* **1976**, *59*, 1099. (c) Yam, V. W. W.; Lee, V. W. M.; Ke, F.; Siu, M. K. W. *Inorg. Chem.* **1997**, *36*, 2124.